

Effects of 5d Ir-substitution on structures, transport and magnetic properties of $\text{Sr}_2\text{FeMoO}_6$

Jin-Feng Wang^a, Zheng Li^a, Shan-Tao Zhang^{a,*}, Jian Zhou^a, Zheng-Bin Gu^a, Shu-Hua Yao^a, Y.B. Chen^b, Yan-Feng Chen^a

^aNational Laboratory of Solid State Microstructure and Department of Materials Science and Engineering, Nanjing University, Hankou Road, Nanjing 210093, China

^bNational Laboratory of Solid State Microstructure and Department of Physics, Nanjing University, Nanjing 210093, China

Received 13 December 2012; received in revised form 21 December 2012; accepted 21 December 2012

Available online 11 January 2013

Abstract

$\text{Sr}_2\text{Fe}_{1-0.5x}\text{Mo}_{1-0.5x}\text{Ir}_x\text{O}_6$ ceramics ($x=0, 0.02, 0.04, 0.06, \text{ and } 0.08$) have been synthesized and the structures, magnetic and transport properties have been investigated. X-ray diffraction reveals a very low solution limit of $x=0.06$, which however, results in significantly decreased Fe/Mo ordering degree and thus decreased magnetization value. On the other hand, the Curie temperature (T_c) rises from 390 K ($x=0$) to 400 K ($x=0.02$) firstly, and then decreases to 360 K and 340 K for the compositions with $x=0.04$ and 0.06, respectively. In addition, the resistivity and magnetoresistance drop drastically with increasing x . The composition with $x=0$ shows semiconductor transport behavior in the temperature range of 10–400 K, whereas the other compositions show a minimum resistivity around 120 K. These results are discussed in detail by considering the effects of Ir substitution.

© 2013 Elsevier Ltd and Techna Group S.r.l. All rights reserved.

Keywords: B. Ir-substitution; C. Magnetoresistance; D. Double perovskite

1. Introduction

As a representative of the double perovskite oxides with the general formula of $\text{A}_2\text{B}'\text{B}''\text{O}_6$ (where A is an alkaline-earth or rare-earth cation and B is a transitional metal cation), ferrimagnetic $\text{Sr}_2\text{FeMoO}_6$ (SFMO) has been reported firstly for the anomalous magneto-optical Kerr effect and then extensively been investigated for the intrinsic room temperature tunneling-type magnetoresistance (MR) [1–3]. Along with its half metal characteristics and high Curie temperature ($T_c \sim 415$ K) [2,4], SFMO is attractive not only for fascinating physics but also for potential applications in spintronic devices, etc., operated at room temperature [5].

Ideally, Sr cation occupies the A site, while Fe and Mo cations occupy the B (B' and B'') sites alternatively. The antiferromagnetical coupling between Mo^{5+} and Fe^{3+} leads to a magnetization (M_s) of $4 \mu_B$ per formula cell (f.u.).

Therefore, it is reasonable that M_s strongly depends on the ordering degree of Fe/Mo. Indeed, weakened magnetization is commonly found due to the appearance of the so called antisite defects (ASD, which is the occupying Fe sites by Mo and *vice versa*) [6–8]. ASD is very sensitive to any B-site substitutions, which means that B-site substitutions can tune the ASD concentration, and thus the physical properties. Accordingly, great efforts have been devoted to such substitutions to explore and tune the B-site ordering degree and the corresponding magnetic properties. Up to now, works on B-site substituted SFMO mainly focus on nonmagnetic or magnetic elements such as Al, Cu, Ni, Cr, Sc, Ti, V, etc., substituting for Fe [4,9–13]. It is noted that most of these substituting elements belong to the 3d transition metal family.

On the other hand, it is well known that 5d transition metal elements based perovskite oxides may have rich physical properties, mainly due to the spatially more extended 5d orbital and relatively larger spin–orbit coupling. Actually, some 5d element based double perovskite oxides, where B'' = Re, W, Os, Ir, etc., have been reported and various

*Corresponding author. Tel.: +86 25 83594317.

E-mail address: stzhang@nju.edu.cn (S.-T. Zhang).

magnetic behaviors like paramagnetism, antiferroelectricism and ferromagnetism observed [4,14–17]. This means substituting Fe/Mo (which are 3d and 4d transition metal elements, respectively) by 5d elements may be a promising method to tune the fundamental physics of SFMO. It is expected that such 5d element substituted 3d and 4d-based double perovskites may also have some unusual behaviors, which are very rare in literatures. One example is the W-substituted SFMO where the 5d W element substitutes for the 4d Mo [18,19]. The W^{6+} ($5d^0$, $s=0$) can suppress the Fe^{3+} ($3d^5$, $s=5/2$) state to become the Fe^{2+} ($3d^6$, $s=2$) state partially, and as the result, W-substitution reinforces the B site ordering degree to some extent and changes the crystal structure from cubic to the tetragonal, therefore, the materials transfer from ferromagnetic metal to antiferromagnetic insulator and both the Curie temperature and the magnetization are improved [18,19].

Encouraged by the nonmagnetic 5d W^{6+} ($5d^0$, $s=0$) substituted SFMO and by further noticing that the 5d Ir^{4+} cation is magnetic ($5d^5$, $s=1/2$) and has definitely non-equal valence with Fe^{3+}/Mo^{5+} [20], in this paper, we have prepared and systematically investigated the structures, magnetic and electronic transport properties of $Sr_2Fe_{1-0.5x}Mo_{1-0.5x}Ir_xO_6$ ($x=0, 0.02, 0.04, \text{ and } 0.06$) ceramics. The effects of Ir substitution on the structures and physical properties have been discussed in detail.

2. Experimental

Polycrystalline samples of $Sr_2Fe_{1-0.5x}Mo_{1-0.5x}Ir_xO_6$ ($x=0, 0.02, 0.04, 0.06$ and 0.08), abbreviated as S1, S2, S3, S4, S5,

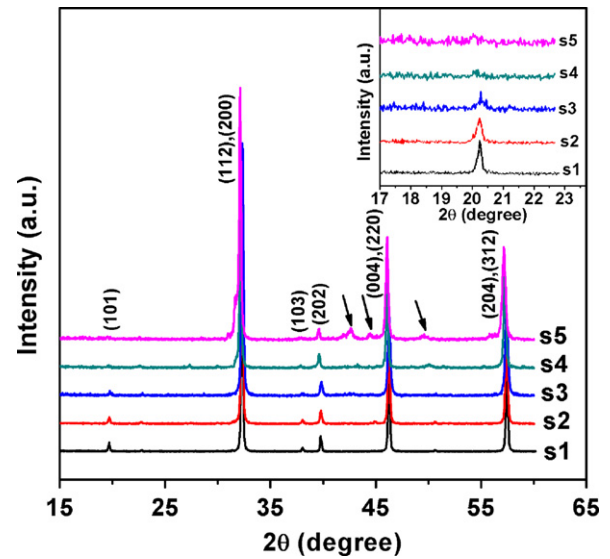


Fig. 1. X-ray diffraction profiles of as-obtained $Sr_2(FeMo)_{1-x}Ir_xO_6$ ($x=0, 0.02, 0.04, 0.06$ and 0.08) ceramics.

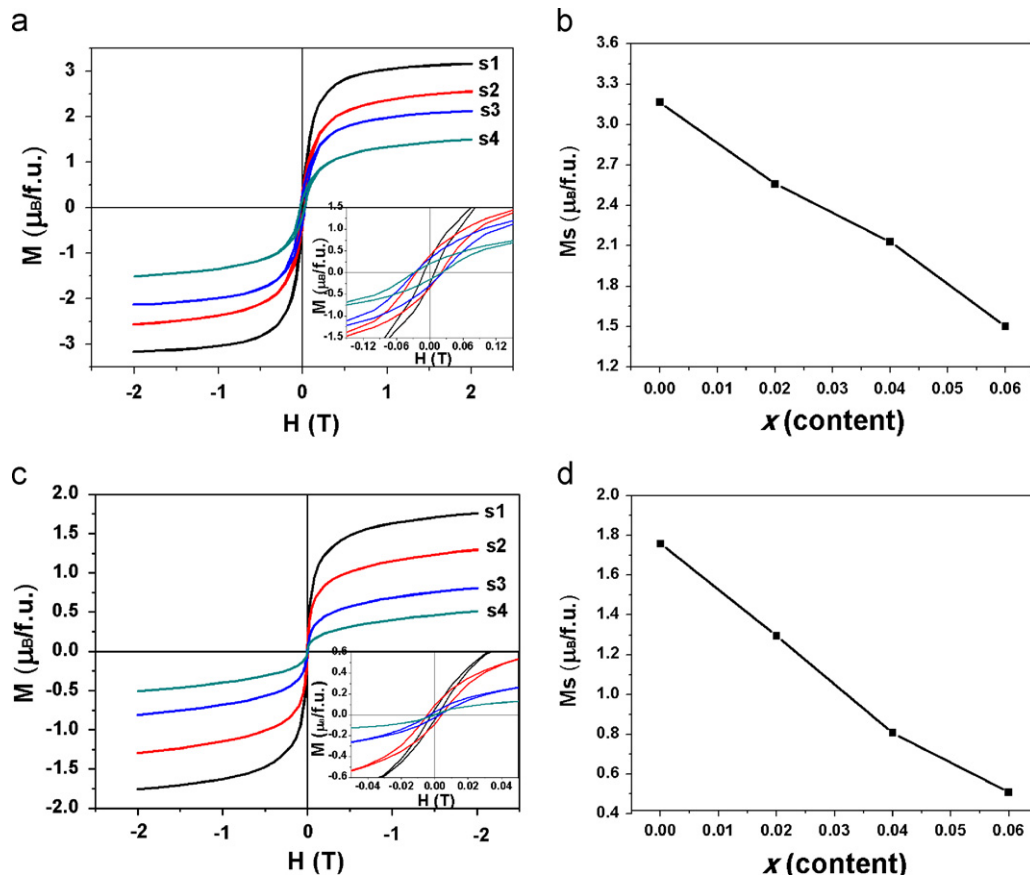


Fig. 2. Magnetization (M – H) curves at 10 K (a) and 300 K (c), the inset present partially enlargement curves. The dependence of M_s on Ir concentration at 10 K (b) and 300 K (d).

S4 and S5, respectively, were synthesized by solid-state reaction [21]. Firstly, stoichiometric amounts of SrCO_3 , Fe_2O_3 , MoO_3 and IrO_2 (analytical grade) were weighed, ball milled in ethanol for 20 h, and dried. The dried powders were calcined at 1073 K for 5 h in air. Subsequently, the powders were ball milled again for 20 h, dried, pressed into rectangle slices ($10 \text{ mm} \times 5 \text{ mm} \times 0.5 \text{ mm}$). At last, sintering was carried out under flowing mixed gas of 5% $\text{H}_2 + 95\% \text{ Ar}$. The S1 was sintered at 1473 K for 12 h while other samples at 1373 K for 6 h. It should be mentioned the sintering temperature and dwell time for each composition have been optimized based on our systematical experiments.

The structures of the samples were characterized through X-ray diffraction (XRD) patterns (Rigaku Ultima III). The magnetic and transport data were collected by using a superconductor quantum interference device (SQUID, Quantum Design, MPMS XL-7) and a physical property measurements system (PPMS Quantum Design, 2001NUGC).

3. Results and discussion

Fig. 1 shows the XRD patterns of all the samples. It can be seen that for each composition, all the diffraction peaks are in good agreement with the double perovskite structure with tetragonal structure (space group $I4/mmm$) [22]. However, for S5 has some impurity phases such as cubic Fe, as indicated by the arrows. Actually, in our experiments, single phase S5 can not be obtained within a wide sintering temperature range (from 1173 K to 1573 K) and dwell time range (from 2 h to 30 h), so it may be safe to conclude that the substitution limit of Ir into SFMO is only about 0.06, which is far lower than other B-sites substituted SFMO, as summarized in Ref. [5]. However, our observation is reasonable because perovskite orthorhombic SrIrO_3 is metastable under ambient condition [23,24], this might mean that the introduction of Ir into the lattice of SFMO may cause local lattice distortion or structure instability, thus leads to the formation of second phases. In the following sections, our discussions will focus on single phase ceramics of S1, S2, S3 and S4.

The inset of Fig. 1 presents the locally enlarged XRD patterns of the samples. The (101) diffraction peak around $2\theta = 19.8^\circ$ is generally identified as the superstructure peak, and the intensity ratio of $I(101)/(I(112)+I(200))$ indicates the Fe/Mo ordering degree [10]. As can be seen, with increasing Ir content (x) from 0 to 0.06, the superstructure diffraction intensity is suppressed dramatically, and the superstructure diffraction peak tends to disappear when x reaches 0.06. This means the Ir substituting can decrease the cation ordering degree, or increase the ASD concentration. Actually, based on the following magnetic measurements, the ASD concentration is estimated to increase from 10.3% for $x=0$ to 27.4% for $x=0.06$ by using the empirical formula of $M_s = 4.04 - 8.1(8)x$, where x is the ASD concentration [25]. Such dramatically increased ASD may come from the following two aspects: On the one hand, the Ir-substitution can break the alternative arrangement of Fe and Mo cations and thus increases such substitution-induced ASD. However, this contribution should

not be so significant because the substitution level is considerably low ($x \leq 0.06$). On the other hand, the valence difference between cations can also increase ASD. As well known, larger valence difference between B'' and B' favors the formation of higher cation order in SFMO [26]. However, in our case the valence difference between Ir^{4+} and $\text{Fe}^{3+}/\text{Mo}^{5+}$ is 1, which is smaller than 2 between Fe^{3+} and Mo^{5+} .

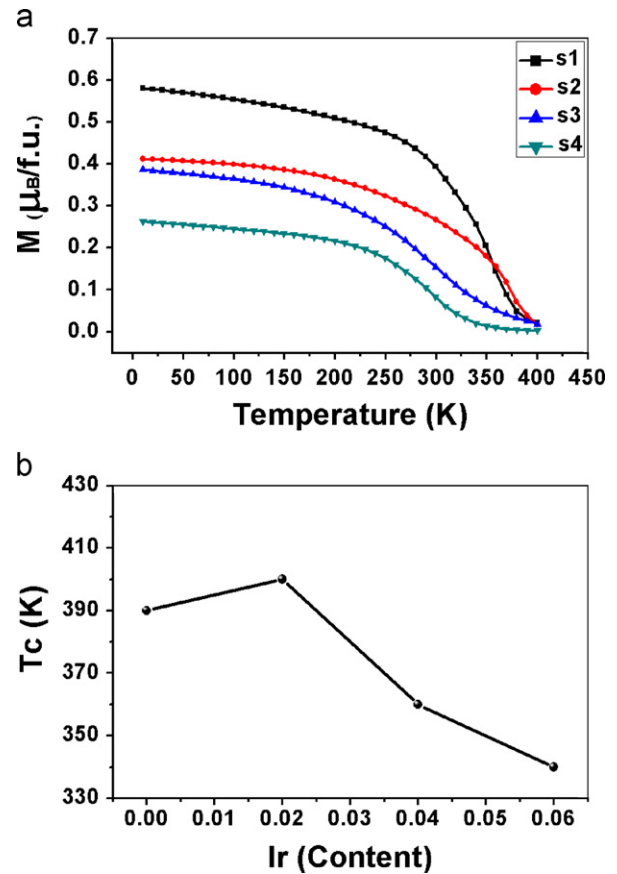


Fig. 3. Temperature dependent magnetization of $\text{Sr}_2(\text{FeMo})_{1-x}\text{Ir}_x\text{O}_6$ ($0 \leq x \leq 0.06$) (a), and (b) variation of the curie temperature, T_c with Ir composition.

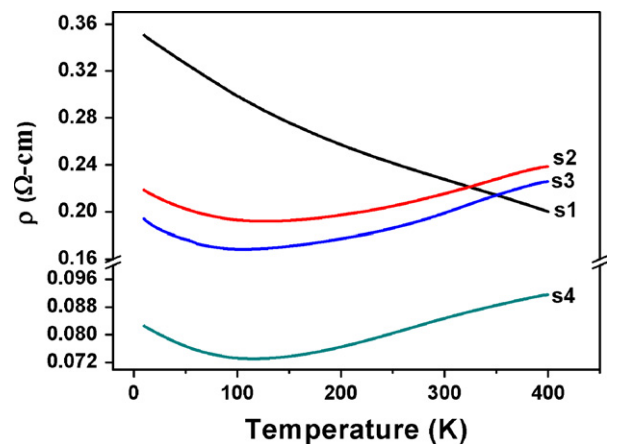


Fig. 4. Temperature dependence of electrical resistivity of $\text{Sr}_2(\text{FeMo})_{1-x}\text{Ir}_x\text{O}_6$ ($0 \leq x \leq 0.06$) ceramic pellets in zero field.

Magnetization–magnetic field (M – H) curves recorded at 10 K and room temperature (RT) are depicted in Figs. 2(a) and (c), respectively. The insets show the corresponding locally enlarged curves. As can be seen from Fig. 2(a), all the compositions show well-saturated M – H hysteresis loops, exhibiting a feature of the macroscopic ferromagnetic behavior. With increasing x , the values of saturated magnetization (M_s) at 10 K and RT decrease almost linearly, as plotted in Figs. 2(b) and (d), respectively. Of particular interest is that the coercive field (H_c) of S2, S3 and S4 are comparable but larger than that of S1, as shown in the inset of Fig. 2(a), similar result is also observed at RT (the inset of Fig. 2(c)).

The magnetic observations in Fig. 2 can be rationalized as the follows: according to the XRD patterns, the ASD concentration increases with increasing x . And it is reported that M_s has an almost linear dependence on the ASD concentration, $M_s=4.04-8.1(8)x$, where x is the ASD concentration [25], which is again confirmed by our observations. The magnetic hardening might be attributed to that more ASD leads to the presence of more anti-ferromagnetic (AF)

patches, thus magnetic domain rotation process is more difficult [26,27].

Fig. 3(a) plots the field-cooling (200 Oe) magnetization–temperature (M – T) curves for all the samples. With increasing temperature, the samples exhibit a transition from paramagnetic to ferromagnetic phase. The transition temperatures T_c are plotted against x value and shown in Fig. 3(b). It is interesting to find that the T_c (400 K) of S2 is relatively higher than that of S1 (390 K) in spite of the fact that the ASD in S2 is a little more than that in S1 (Fig. 1). This observation can be related to the effect of oxygen deficiency which is extremely sensitive to sintering process. As shown above, both the sintering temperature and dwell time of S2 are lower than that of S1, so it is reasonable that S2 may have less oxygen vacancy than S1, less oxygen vacancy generally can promote ferromagnetic interactions and improve T_c [28]. Although S3 and S4 may also have less oxygen vacancy, the detrimental effect of ASD on property is enhanced and tend to be dominant [29,30], so S3 and S4 have decreased T_c of 360 K and 340 K, respectively.

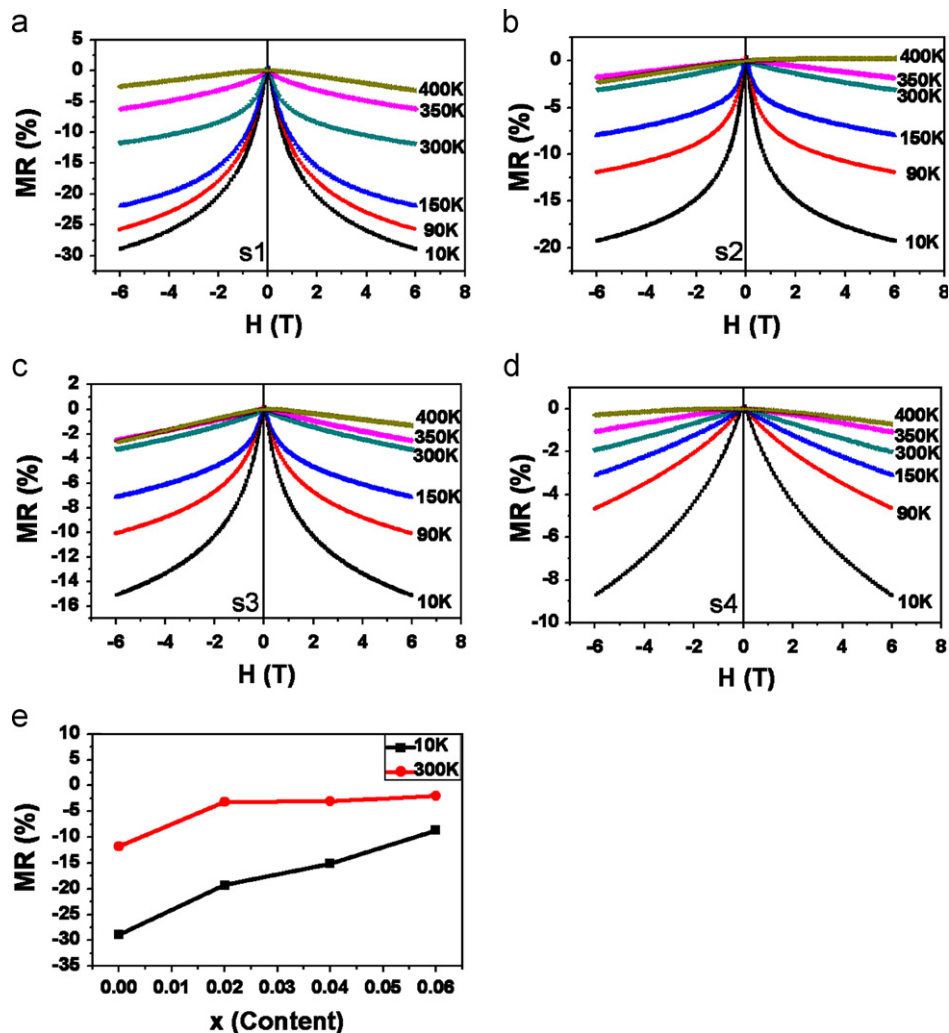


Fig. 5. Magnetoresistance for $\text{Sr}_2(\text{FeMo})_{1-x}\text{Ir}_x\text{O}_6$ at different temperatures (a) $x=0$, (b) $x=0.02$, (c) $x=0.04$, (d) $x=0.06$, and (e) the composition MR measured with 6 T at 10 K and RT .

Fig. 4 describes the temperature dependence of the resistivity for all the samples. It is obvious that S1 exhibits a semiconductor-like behavior in the whole measured temperature range (10–400 K), i.e., the resistivity decreases gradually with increasing temperature. However, for the other three samples, on the one hand, the resistivity values decrease gradually with increasing of Ir content, especially the resistivity of the S4 is far lower than that of S1. The substitution-decreased resistivity may be ascribed to the spatially more extended 5d orbits of Ir, which facilitates the hopping of electrons [31]. On the other hand, it is interesting to notice that all Ir-substituted SFMO (S2, S3, S4) exhibit semiconductor behavior until a minimum resistivity around 120 K is reached, and then metal behavior above 120 K, which has no apparent composition dependence. Similar results were reported in $\text{Sr}_2(\text{Fe}_{1-x}\text{Cu}_x)\text{MoO}_6$ [13], which indicates a possible semiconductor-to-metal transition like behavior. However, based on the thermal variation of resistivity, we cannot exclude Kondo-like behavior, as typically found in manganites [32,33], where interplay between electron–electron, electron–phonon, and electron–magnon scattering leads to the minimum in the temperature dependence of resistivity. Actually, the extended orbital of Ir may enhance these interactions. To classify the origination of the composition dependent resistivity and the minimum resistivity, further detailed works are necessary and underway.

Field-dependent magnetoresistance (MR) for all the samples are measured at different temperatures, as shown in Figs. 5(a)–(d). The MR ratio is defined as $\text{MR}(\%) = (R_{\text{H}} - R_0)/R_0 \times 100\%$, where R_0 and R_{H} are the resistivity values at zero and 2 T applied magnetic fields, respectively. Three features about the MR curves should be mentioned. Firstly, the MR value is close to zero when measured at 400 K, which is attributed to the almost disappear of magnetic ordering. With decreasing measuring temperature, the MR values of all samples increase. Secondly, for each sample, the MR values measured with fixed temperature increase with increasing magnetic field. Interestingly, the negative MR increases more abruptly in the low field region than in the high field region, as indicated by the steep magnetization process, which actually is the characteristic of low-field magnetoresistance effect [34]. Thirdly, it is noted that with increasing x , the MR values decrease almost linearly. The typical MR values of all samples measured at 6 T at 10 K and 300 K are plotted in Fig. 5(e). This linear dependence of MR on x value is consistent with the linear dependence of magnetization on x value. This is reasonable since the hopping of spin-polarized electrons can be affected by magnetic domains. Actually, similar magnetization-dependent MR behavior can be found in other reports [26,27].

4. Conclusion

In summary, single phase Ir-substituted SFMO, i.e. $\text{Sr}_2\text{Fe}_{1-0.5x}\text{Mo}_{1-0.5x}\text{Ir}_x\text{O}_6$, ceramics have been prepared. XRD analysis confirms that the low solution limit is $x=0.06$. Substitution of Ir in SFMO can increase the

ASD concentration and result in a decrease of magnetization and magnetoresistance. However, Ir substitution can improve the conductivity of SFMO. We hope our results can stimulate further work on 5d transition metal based double perovskite.

Acknowledgments

This work was supported by the National Key Basic Research Program of China (2013CB632904 and 2013CB632702), the National Nature Science Foundation of China (11174127, 11134006), and the Doctoral Fund of Ministry of Education of China (20110091110014).

References

- [1] H. Matsushima, H. Gotoh, Y. Takeda, K. Ueda, H. Asano, Magnetic and Electronic Properties of Double Perovskite $\text{Sr}_{2-x}\text{La}_x\text{VMoO}_6$, *Japanese Journal of Applied Physics* 50 (2011) 103004.
- [2] K.L. Kobayashi, T. Kimura, H. Sawada, K. Terakura, Y. Tokura, Room-temperature magnetoresistance in an oxide material with an ordered double-perovskite structure, *Nature* 395 (1998) 677.
- [3] G.Y. Huo, J.J. Wen, C.H. Zhang, M.H. Ren, Effect of oxygen substitution by nitrogen on magnetic and transport properties in $\text{Sr}_2\text{FeMoO}_6$ compound, *Ceramics International* 38 (2012) 1359.
- [4] I. Zutic, J. Fabian, S.D. Sarma, *Spintronics: fundamentals and applications*, *Reviews of Modern Physics* 76 (2004) 323.
- [5] D. Serrate, J.M. De Teresa, M.R. Ibarra, Double perovskites with ferromagnetism above room temperature, *Journal of Physics: Condensed Matter* 19 (2007) 023201.
- [6] J.M. Greneche, M. Venkatesan, R. Suryanarayanan, J.M.D. Coey, Mossbauer spectrometry of A_2FeMoO_6 (A=Ca,Sr,Ba): search for antiphase domains, *Physical Review B* 63 (2001) 174403.
- [7] R.P. Borges, R.M. Thomas, C. Cullinan, J.M.D. Coey, R. Suryanarayanan, L. Ben-Dor, L. Pinsard-Gaudart, A. Revcolevschi, Magnetic properties of the double perovskites A_2FeMoO_6 ; A=Ca, Sr, Ba, *Journal of Physics: Condensed Matter* 11 (1999) L445.
- [8] T.H. Kim, M. Uehara, S.W. Cheong, S. Lee, Large room-temperature intergrain magnetoresistance in double perovskite $\text{SrFe}_{1-x}(\text{Mo}/\text{Re})_x\text{O}_3$, *Applied Physics Letters* 74 (1999) 1737.
- [9] A. Pena, J. Gutierrez, L.M. Rodriguez-Martinez, J.M. Barandiaran, T. Hernandez, T. Rojo, Structure and magnetism in $\text{Sr}_2(\text{Fe}_{1-x}\text{Al}_x)\text{MoO}_6$ ($0 \leq x \leq 0.3$) double perovskite compounds, *Journal of Physics: Condensed Matter* 13 (2001) 6535.
- [10] Y. Sui, X.J. Wang, Z.N. Qian, J.G. Cheng, Z.G. Liu, J.P. Miao, Y. Li, W.H. Su, C.K. Ong, Enhancement of low-field magnetoresistance in polycrystalline $\text{Sr}_2\text{FeMoO}_6$ with Al doping, *Applied Physics Letters* 85 (2004) 269.
- [11] A. Gaur, G.D. Varma, H.K. Singh, Enhancement in Curie temperature and reduction in magnetoresistance of $\text{Sr}_2(\text{Fe}_{1-x}\text{Ni}_x)\text{MoO}_6$ ($0 \leq x \leq 0.15$), *Journal of Alloys and Compounds* 460 (2008) 581.
- [12] J.H. Kim, G.Y. Ahn, S.I. Park, C.S. Kim, Effects of Cr doping on magnetic properties of ordered $\text{Sr}_2\text{FeMoO}_6$, *Journal of Magnetism and Magnetic Materials* 282 (2004) 295.
- [13] G.L. Yuan, Y. Zhu, P.P. Ong, Effect of Cu doping on the magnetoresistive behavior of double perovskite $\text{Sr}_2\text{FeMoO}_6$ polycrystals, *Journal of Applied Physics* 91 (2002) 4421.
- [14] C. Azimonte, J.C. Cezar, E. Granado, Q. Huang, J.W. Lynn, J.C.P. Campoy, J. Gopalakrishnan, K. Ramesha, Incipient orbital order in half-metallic $\text{Ba}_2\text{FeReO}_6$, *Physical Review Letters* 98 (2007) 017204.

- [15] H. Das, M. De Raychaudhury, T. Saha-Dasgupta, Moderate to large magneto-optical signals in high T_c double perovskites, *Applied Physics Letters* 92 (2008) 201912.
- [16] A.S. Erickson, S. Misra, G.J. Miller, R.R. Gupta, Z. Schlesinger, W.A. Harrison, J.M. Kim, I.R. Fisher, Ferromagnetism in the Mott insulator Ba₂NaOsO₆, *Physical Review Letters* 99 (2007) 016404.
- [17] N. Narayanan, D. Mikhailova, A. Senyshyn, D.M. Trots, R. Laskowski, P. Blaha, K. Schwarz, H. Fuess, H. Ehrenberg, Temperature and composition dependence of crystal structures and magnetic and electronic properties of the double perovskites La_{2-*x*}Sr_{*x*}CoIrO₆ (0 ≤ *x* ≤ 2), *Physical Review B* 82 (2010) 024403.
- [18] J. Linden, T. Yamamoto, J. Nakamura, M. Karppinen, H. Yamauchi, Coexistence of intrinsic and extrinsic magnetoresistance in the double-perovskite Sr₂Fe(Mo_{1-*x*}W_{*x*})O₆ system, *Applied Physics Letters* 78 (2001) 2736.
- [19] K.I. Kobayashi, T. Okuda, Y. Tomioka, T. Kimura, Y. Tokura, Possible percolation and magnetoresistance in ordered double perovskite alloys Sr₂Fe(W_{1-*x*}Mo_{*x*})O₆, *Journal of Magnetism and Magnetic Materials* 218 (2000) 17.
- [20] H. Watanabe, T. Shirakawa, S. Yunoki, Microscopic study of a spin-orbit-induced Mott insulator in Ir oxides, *Physical Review Letters* 105 (2010) 216410.
- [21] S. Middey, S. Jana, S. Ray, Surface spin-glass and exchange bias in Sr₂FeMoO₆ nanoparticle, *Journal of Applied Physics* 108 (2010) 043918.
- [22] D.D. Sarma, S. Ray, K. Tanaka, M. Kobayashi, A. Fujimori, P. Sanyal, H.R. Krishnamurthy, C. Dasgupta, Intergranular magnetoresistance in Sr₂FeMoO₆ from a magnetic tunnel barrier mechanism across grain boundaries, *Physical Review Letters* 98 (2007) 157205.
- [23] K. Ohgushi, H. Gotou, T. Yagi, Y. Kiuchi, F. Sakai, Y. Ueda, Metal-insulator transition in Ca_{1-*x*}Na_{*x*}IrO₃ with post-perovskite structure, *Physical Review B* 74 (2006) 241104.
- [24] J.G. Zhao, L.X. Yang, Y. Yu, F.Y. Li, R.C. Yu, Z. Fang, L.C. Chen, C.Q. Jin, High-pressure synthesis of orthorhombic SrIrO₃ perovskite and its positive magnetoresistance, *Journal of Applied Physics* 103 (2008) 103706.
- [25] L. Balcells, J. Navarro, M. Bibes, A. Roig, B. Martinez, J. Fontcuberta, Cationic ordering control of magnetization in Sr₂FeMoO₆ double perovskite, *Applied Physics Letters* 78 (2001) 781.
- [26] F. Sher, A. Venimadhav, M.G. Blamire, K. Kamenev, J.P. Attfield, Cation size variance effects in magnetoresistive Sr₂FeMoO₆ double perovskites, *Chemistry of Materials* 17 (2005) 176.
- [27] M. Garcia-Hernandez, J.L. Martinez, M.J. Martinez-Lope, M.T. Casais, J.A. Alonso, Finding universal correlations between cationic disorder and low field magnetoresistance in FeMo double perovskite series, *Physical Review Letters* 86 (2001) 2443.
- [28] R. Mishra, O.D. Restrepo, P.M. Woodward, W. Windl, First-principles study of defective and nonstoichiometric Sr₂FeMoO₆, *Chemistry of Materials* 22 (2010) 6092.
- [29] R.P. Panguluri, S. Xu, Y. Moritomo, I.V. Solovyev, B. Nadgorny, Disorder effects in half-metallic Sr₂FeMoO₆ single crystals, *Applied Physics Letters* 94 (2009) 012501.
- [30] J. Navarro, J. Nogues, J.S. Munoz, J. Fontcuberta, Antisites and electron-doping effects on the magnetic transition of Sr₂FeMoO₆ double perovskite, *Physical Review B* 67 (2003) 174416.
- [31] J.G. Cheng, J.S. Zhou, J.B. Goodenough, Y. Sui, Y. Ren, M.R. Suchomel, High-pressure synthesis and physical properties of perovskite and post-perovskite Ca_{1-*x*}Sr_{*x*}IrO₃, *Physical Review B* 83 (2011) 064401.
- [32] D. Kumar, J. Sankar, J. Narayan, R.K. Singh, A.K. Majumda, Low-temperature resistivity minima in colossal magnetoresistive La_{0.7}Ca_{0.3}MnO₃ thin films, *Physical Review B* 65 (2002) 094407.
- [33] D.S. Rana, J.H. Markna, R.N. Parmar, D.G. Kuberkar, P. Raychaudhuri, J. John, S.K. Malik, Low-temperature transport anomaly in the magnetoresistive compound (La_{0.5}Pr_{0.2})Ba_{0.3}MnO₃, *Physical Review B* 71 (2005) 212404.
- [34] V. Pandey, V. Verma, G.L. Bhalla, R.K. Kotnala, Increased low field magnetoresistance in electron doped system Sr_{0.4}Ba_{1.6-*x*}La_{*x*}FeMoO₆, *Journal of Applied Physics* 108 (2010) 053912.